



Effect of periodic horizontal gradients on the retrieval of atmospheric profiles from occultation measurements

Bachir Belloul, Alain Hauchecorne

► To cite this version:

Bachir Belloul, Alain Hauchecorne. Effect of periodic horizontal gradients on the retrieval of atmospheric profiles from occultation measurements. Radio Science, 1997, 32 (2), pp.469-478. 10.1029/96RS03599 . insu-03580844

HAL Id: insu-03580844

<https://insu.hal.science/insu-03580844>

Submitted on 19 Feb 2022

HAL is a multi-disciplinary open access archive for the deposit and dissemination of scientific research documents, whether they are published or not. The documents may come from teaching and research institutions in France or abroad, or from public or private research centers.

Copyright

L'archive ouverte pluridisciplinaire **HAL**, est destinée au dépôt et à la diffusion de documents scientifiques de niveau recherche, publiés ou non, émanant des établissements d'enseignement et de recherche français ou étrangers, des laboratoires publics ou privés.

Effect of periodic horizontal gradients on the retrieval of atmospheric profiles from occultation measurements

M. B. Belloul and A. Hauchecorne

Service d'Aéronomie, Centre National de la Recherche Scientifique, Verrières le Buisson, France

Abstract. Spherical symmetry is generally assumed during the retrieval process of atmospheric profiles from occultation measurements. The existence of periodic horizontal gradients, occurring on scales comparable to the distances traveled by the rays around their tangent point, is produced by gravity waves. These waves can introduce density perturbations of up to 1 or 2% in amplitude and affect the retrieved parameters accordingly. We show the consequences of ignoring these gradients in the retrieved refractivity profiles when spherical symmetry is assumed. We find that only the waves, with horizontal wavelengths close to the horizontal distance that rays travel in their final 6 or 8 km in the vertical before they are tangent in the atmosphere, will have an influence on the retrieved profiles by introducing a phase delay in the local profile of the retrieved refractivity. The horizontal wavelength of these waves corresponds to the minimum horizontal resolution associated with the retrieved profiles. We also find that smaller scale waves do not have any significant impact on the retrieved profiles, as their contribution cancels out by averaging through the periodic perturbation, while waves with very long horizontal wavelengths are in good agreement with a local spherical symmetry assumption.

Introduction

Progress in satellite technology achieved in the early 1970s and the possibility of sounding the atmosphere of planets from space have given atmospheric sensing another dimension. Since then, occultation techniques have been used to infer precious information about the internal structure, composition, and density profiles of constituents of the atmosphere [Roble and Hays, 1972]. These techniques, which associate sources such as the Sun, stars, or artificial satellites to a ground-based or spaceborne receiver, have enabled sounding of Earth's atmosphere [Rangaswamy, 1976; Kursinski et al., 1996] as well as those of remote planets [Fjeldbo and Von Eshelman, 1968; Fjeldbo et al., 1971; Lindal et al., 1983, 1987]. Modern technology has contributed a great deal to improving the vertical resolution of the retrieved data by yielding better accuracy of the position and velocity components of the satellites involved in the occultation and by allowing the possibility of increasing the sampling rates as well as reducing receiver noise to acceptable levels.

Copyright 1997 by the American Geophysical Union.

Paper number 96RS03599.
0048-6604/97/96RS-03599\$11.00

Figure 1 illustrates a satellite to satellite occultation where the receiver is located on a low Earth orbit spacecraft, while the source is at a much greater altitude. As the receiving satellite progresses in its orbit, the source ultimately is occulted by the atmosphere. During the occultation, the setting (or rising) of the receiver allows a vertical scanning of the atmosphere, which provides a sounding of its total thickness at the vertical of the ray perigee. Observations made during occultation experiments either consist of the excess Doppler shift of the received signal caused by the atmospheric delay or the signal attenuation, both of which are caused by changes in the properties of the medium sustaining the propagation. The excess Doppler shift can also be expressed in terms of the angle of refraction of the ray from its direction in the vacuum. According to Lusignan et al. [1969], the horizontal component of the gradient of refractivity normal to the occultation plane defined by the source, the receiver, and the Earth center (Figure 1) has very little effect on the rays, so that the bending remains principally dominated by the gradients in the plane of occultation. Although sounding generally integrates information in two directions, along the limb and across it as a result of the receiver's motion around its orbit, the resulting atmospheric profiles are generally credited to a single direction, i. e., at the vertical of the ray perigee. In order to yield the atmospheric parameter under investigation,

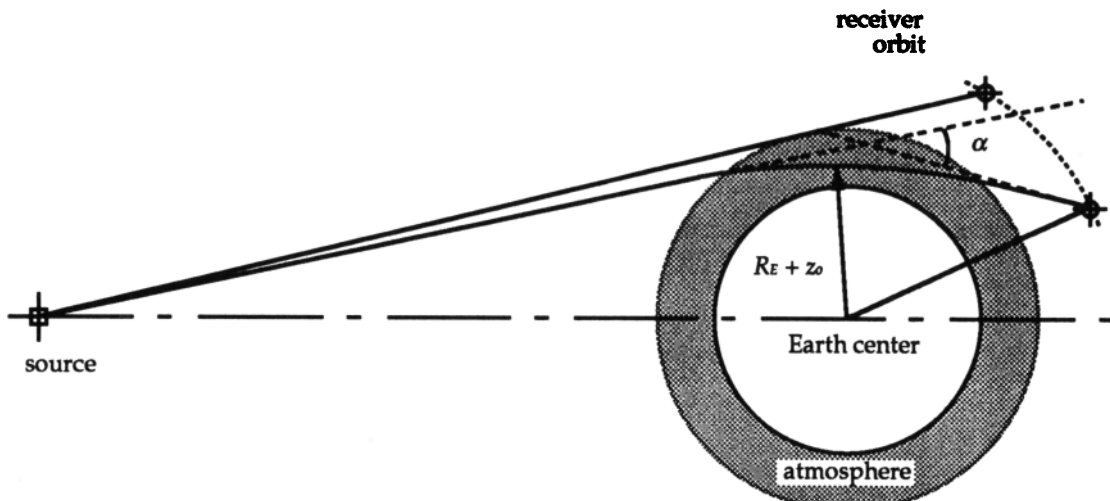


Figure 1. Geometry of a satellite to satellite occultation.

it is necessary to solve the inverse problem. When the measured profile is inverted to restore the local propagation conditions, it is generally essential to speculate on the properties of the medium causing the measured observations. The hypothesis that is generally made is to assume that the atmosphere is locally in spherical symmetry about the Earth center. In most occultation problems, this hypothesis remains appropriate with regard to the accuracy with which the atmospheric profiles are to be retrieved and is particularly true for remote planets where only scarce measurements are available. However, the existence of horizontal gradients in the atmosphere can induce discrepancies in resulting observations that need to be addressed if accurate retrievals are required. This problem was investigated by *Gorbunov* [1990] who treated inhomogeneities with a small perturbation method. *Lindal* [1992] also looked at the case where the gravity field was not spherically uniform but presented a significant tilt caused by the planet's oblateness. In this paper, we evaluate the effects of periodic perturbations of the horizontal density field such as those that gravity waves (GWs) can produce on the retrieval of atmospheric profiles.

According to Figure 1, a ray that reaches its perigee at 40 km would have traveled approximately 500 km along the horizontal in Earth's neutral atmosphere during the last 10 km (in vertical distance) prior to perigee point. GWs of this scale appear to be a common feature in the stratosphere, where they have been detected by radar, lidar, and other instruments [*Vincent and Reid*, 1983; *Balsley et al.*, 1983; *Wilson et al.*, 1990]. They play a major role in middle atmosphere dynamics [*Allen and*

Vincent, 1995] and should, for that matter, be considered as an intrinsic part of the atmospheric structure. Gravity waves usually have periods of the order of a few minutes to an hour or so, while their vertical wavelengths range from 1 to 15 km and their horizontal wavelengths range from a few tens to a few thousand kilometers.

The atmosphere has its denser layers nearer the Earth's surface. In the absence of turbulence or inversion layers, the density gradients will be uniformly increasing toward the surface, leading to a greater contribution of the lower layers of the atmosphere to the refraction of the rays. Figure 2 shows the refraction angle, integrated along the path and normalized to the total refraction, for the rays tangent at 20 and 40 km. The contribution of the last 2 km (in vertical distance) prior to the tangent altitude is at least 50% of the total ray bending, while 80% of the total bending results from crossing the last 6 km. The horizontal wavelengths associated with GWs are of comparable scales as the horizontal distance traveled by the rays about the tangent point, where most of the bending is achieved, and it is legitimate therefore to expect some kind of interaction between the GW disturbed atmosphere and the propagating rays. With a simple analytical model for describing the GWs, we estimate the associated effects on the observed profiles of refraction angles. We then perform an inversion of the synthetic refraction angle profiles into refraction index profiles using an Abel inversion [see, for example, *Fjeldbo et al.*, 1971] in order to quantify the consequences of introducing GW induced horizontal gradients in a spherically symmetric atmosphere.

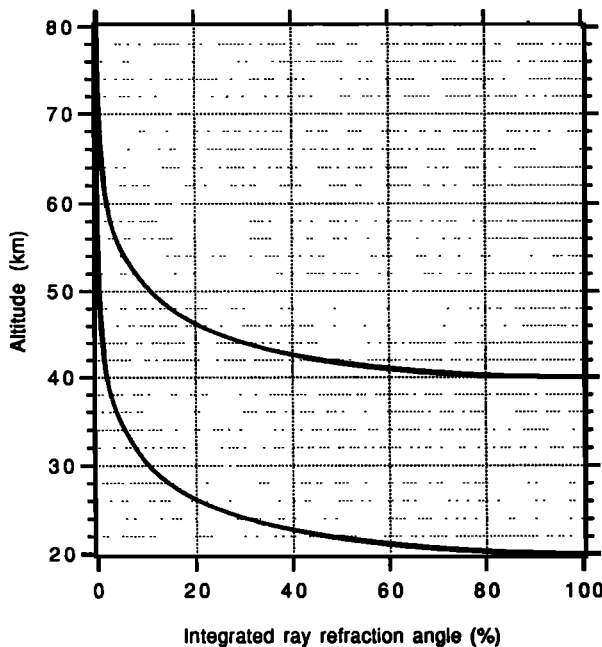


Figure 2. Integrated ray refraction angle versus altitude normalized to the total refraction for the rays tangent at 20 and 40 km.

Refraction Angle Profile in a Nonspherical Atmosphere

During their journey through the atmosphere, electromagnetic rays are subject to phase delays caused by the changes in the refraction index along the path. This effect is also associated with a bending of the ray from the rectilinear direction in the vacuum due to the refraction index gradients, the two effects being linked to each other through the Doppler shift of the frequency. The amount by which the ray is refracted depends on the refraction index distribution in the plane of occultation. In the absence of water vapor and in the radio frequency range, the refractivity N varies linearly with the density ρ (expressed in kilograms per cubic meter) according to

$$N(z) = [n(z) - 1] \cdot 10^6 = 0.776 \rho(z)R \quad (1)$$

where n is the index of refraction and R is the gas constant for dry air.

In this analysis, we assume that atmosphere is isothermal, with a constant density scale height H of 7.5 km. Refractivity perturbations with vertical and horizontal periodicity are mapped onto the isothermal atmosphere in order to represent the effect of the GW. These periodic perturbations introduce horizontal

gradients that are similarly periodic. An analytic solution which satisfies the conditions of propagation of small wave disturbances about a basic state of rest can be written as

$$\frac{dp}{\rho} = W(z) e^{-ik \cdot r} \quad (2)$$

where $W(z)$ is the wave amplitude, k the wavenumber vector and r a position vector. In order to compensate for the decrease in molecular density, the perturbation amplitude normally increases exponentially, with a typical scale height of $2H$. At high altitude, however, the perturbation amplitude should be limited to a maximum of about 2% of the mean density so that the atmosphere remains in adiabatic equilibrium. This was achieved by including a damping term in $W(z)$ that limits the amplitude growth. The time dependence of the wave has been deliberately omitted, as the duration of an occultation in the neutral atmosphere rarely lasts over 1 minute, and one can therefore assume that the waves are motionless during that period.

Applying results from the ray theory to the forward problem, we can reconstruct the trajectories of the rays linking the source with the occulted receiver. The total bending angle of ray that reaches its tangent point at z_o is given by

$$\alpha(z_o) = \int_{\text{ray}} \frac{ds}{R_c} \quad (3)$$

where R_c is the local radius of curvature of the ray and ds is an element of the ray path. The radius of curvature is proportional to the inverse of the refraction index gradient, and for a uniformly decreasing density, it is around the tangent altitude that rays undergo maximum bending. At these altitudes, the angle that makes the trajectory with the local horizontal is never too far from zero and the total bending angle may be approximated by

$$\alpha(z_o) = - \int_{\text{ray}} \frac{1}{n} \frac{dn}{dz} ds \quad (4)$$

For practical reasons, we separate this expression into a mean bending angle $\bar{\alpha}$ induced by the mean density distribution along the ray path and a small disturbance from the mean state α' related to the GWs activity, so that

$$\alpha(z_o) = \bar{\alpha}(z_o) + \alpha'(z_o) \quad (5)$$

In the stratosphere and above, the ray curvature is much smaller than the Earth's curvature. We can therefore derive a first-order relationship between the

horizontal displacement x along the path and its equivalent displacement z in the vertical. In a Cartesian coordinate system and if we assume that the occultation plane containing the ray trajectories is in the $x - z$ plane, this would yield

$$z = z_o + \frac{x^2}{2(R_E + z_o)} \quad (6)$$

where R_E is the local Earth radius. By combining expressions (1), (4), (5) and (6) and retaining only the first-order terms, we end up with an expression for the refraction angle perturbation at a given tangent altitude z_o . After normalizing this perturbation by the total refraction and fixing the tangent point abscissa at $x = 0$, we obtain the expression

$$\alpha'(z_o) = \frac{1}{\sqrt{\pi} \sqrt{2H(R_E + z_o)}} \int_{-\infty}^{+\infty} W e^{-\frac{x^2}{2H(R_E + z_o)}} \left[\sin[\varphi(x) + mz_o] - Hm \cos[\varphi(x) + mz_o] \right] dx \quad (7)$$

where

$$\varphi(x) = kx + m \frac{x^2}{2(R_E + z_o)} \quad (8)$$

is a phase function, and k and m are the horizontal and the vertical wavenumbers, respectively.

The above expression is numerically solved for various GW wavenumbers and a range of tangent altitudes. Only the effects of gravity waves in the neutral atmosphere are considered. The synthetic refraction angle profiles are compared to the profiles obtained when k is set to zero. This condition is a special case corresponding to a spherically symmetric atmosphere.

The variation of α' with altitude, in the range 20 - 26 km and for a selection of horizontal wavelengths and a vertical wavelength $\lambda_v \sim 6.3$ km, is presented in Figure 3, where the solid curve shows the result for $\lambda_h = \infty$. The amplitude of the refractivity perturbation was 1% at these altitudes. For the range of selected horizontal wavelengths, we note that the wavelength of the perturbation is preserved during the forward simulation; but we also notice how the amplitude of the refraction angle perturbation has grown from 1% to about 2 - 3% for the long horizontal wavelengths. The gain in amplitude is mainly due to the fact that the refraction angle is a consequence of the vertical gradients of refractivity rather than the vertical refractivity itself. In order to weight the effects of the GW induced refractivity gradients on the local spherical symmetry, the refraction angle perturbation profiles obtained with the selected values of λ_h should be compared to the

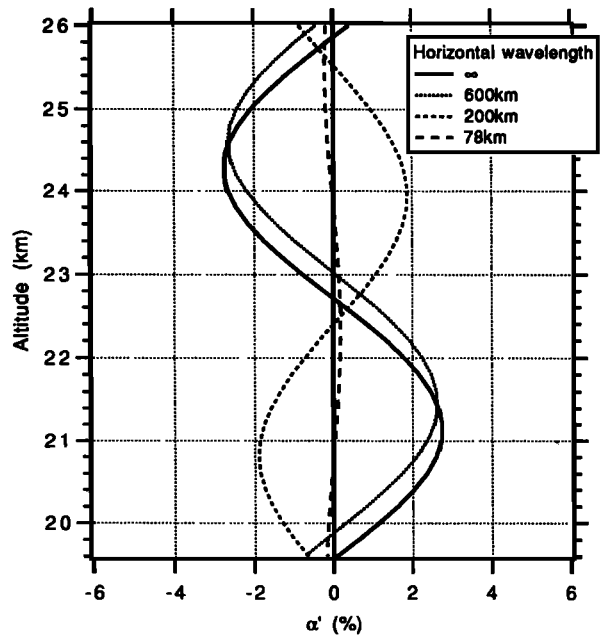


Figure 3. Refraction angle perturbation versus tangent altitude for three horizontal wavelengths and for the spherical symmetry case ($\lambda_h = \infty$). The vertical wavelength of the gravity wave (GW) was fixed at 6.3 km, and its amplitude was 1% at these altitudes.

profile obtained when $\lambda_h = \infty$ ($\alpha'_{k=0}$). For $\lambda_h = 600$ km, for instance, α' and $\alpha'_{k=0}$ profiles are in phase and the values of their amplitudes are similar, suggesting a minor influence of the large waves to alterations in the local spherical symmetry. It follows that the local horizontal gradients induced by the large-scale waves hardly affect the local spherical symmetry and can therefore be dismissed. The scenario becomes different as the horizontal wavelengths progress toward the medium-scale range. For these waves, it appears that the structure of the refraction angle perturbation experiences a phase shift. The phase of $\alpha'(z)$, for instance, is in opposition with the phase of $\alpha'_{k=0}$ when $\lambda_h = 200$ km. This situation means that simulating a refraction angle profile while assuming spherical symmetry, at an altitude where the vertical phase of the GW perturbation corresponds to an amplitude maximum (e.g., at 21.2 km for $\lambda_h \sim 6.3$ km), will result in a maximum error between the real profile and the simulated profile, this error being equal to the difference between $\alpha'_{k=0}$ and α' . The short wave ($\lambda_h = 78$ km), on the other hand, is seen to produce almost no effects at all. The horizontal path length of the ray in the atmospheric layers close to the ray perigee consists of a number of horizontal wavelengths of the GW.

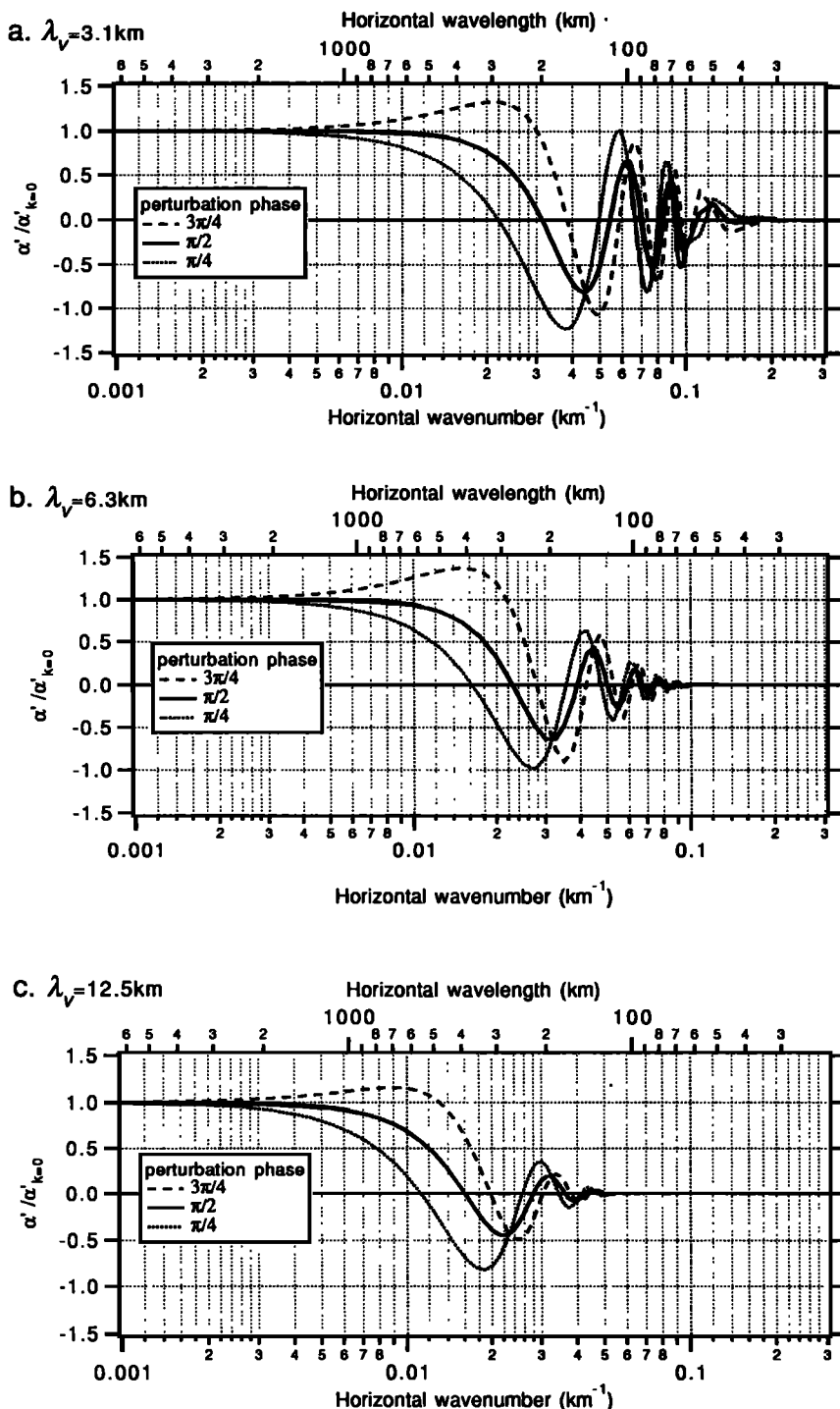


Figure 4. Ratio of the refraction angle perturbation to the refraction angle perturbation for $k = 0$ versus GW horizontal wavelength for three vertical wavelengths, (a) $\lambda_v = 3.1 \text{ km}$, (b) 6.3 km , and (c) 12.5 km . For each λ_v , the ratio is calculated at three tangent altitudes corresponding to $3\pi/4$, $\pi/2$, and $\pi/4$ of the vertical perturbation phase. The amplitude of the GW perturbation was 1% at these altitudes.

Individual contributions from the positive refractivity perturbation regions will, on average, get cancelled out by the contributions from the negative perturbation regions, resulting in a smoothing of the horizontal variability they individually produce.

These observations are better illustrated in Figure 4, where we show the ratio $\alpha'/\alpha'_{k=0}$ between the disturbed cases and the spherical symmetry case for the range of horizontal wavenumbers generally associated with gravity waves. This ratio is calculated for three vertical wavelengths ($\lambda_v = 3.1, 6.3, \text{ and } 12.5 \text{ km}$) at altitudes corresponding to $\pi/4, \pi/2, \text{ and } 3\pi/4$ of the vertical phase of the perturbation. The curves for $\pi/2$ are relative to tangent altitudes where the phase of the perturbation corresponds to an amplitude maximum. These altitudes were situated around 22 - 24 km for the three cases of λ_v . Figure 4 shows that the perturbations generated by the long-scale waves barely produce any difference compared to the perturbation caused by a spherically symmetric atmosphere, as the ratio $\alpha'/\alpha'_{k=0}$ remains close to unity for all horizontal wavelengths greater than $\sim 1000 \text{ km}$. The short waves again give zero perturbation as was stated earlier. In the middle-range domain, we notice, however, that $\alpha'/\alpha'_{k=0}$ goes through a series of oscillations around zero. The amplitude of these oscillations gets damped as the GW horizontal wavenumber increases but they seem to be more persistent for the shortest of the three vertical wavelengths. It is at the peak of the first oscillation that $\alpha'/\alpha'_{k=0}$ reaches its largest negative value, indicating that $\alpha'_{k=0}$ and α' are in phase opposition. The horizontal wavelength at which this occurs increases from approximately 150 km for $\lambda_v = 3.1 \text{ km}$ to 300 km for $\lambda_v = 12.5 \text{ km}$. The amplitude of the first negative oscillation is larger for $\lambda_v = 3.1 \text{ km}$, suggesting that the shorter the vertical wavelengths are (at fixed horizontal wavelength), the more significant effects on the refraction angle will be owing to the greater vertical refractivity gradients associated with these waves.

Retrieved Profiles

Inversion of the $\alpha(z)$ profiles is carried out using an Abel transform, and the retrieved refractivity profiles are compared to the profiles used to simulate the bending angles. The Abel integral, which is an exact solution of the inverse problem, transforms the ray refraction angle profiles into profiles of refraction index at the vertical of the ray perigee, assuming spherical symmetry.

The results of Figure 4 have shown how sensitive radio occultation measurements are to the vertical and the horizontal wavelengths of the GW. In fact, these two parameters determine the spatial distribution of the contours of the atmospheric refractive index gradients.

They have therefore a major influence on the total bending of the radio rays as they locally modulate the ray trajectories. Let us, for that matter, introduce the scaling parameter r_h defined as the ratio of the characteristic horizontal scale $2\sqrt{2}R_E\lambda_v$, equivalent to the horizontal distance traveled by a ray to cover one GW vertical wavelength, divided by the horizontal wavelength of the GW. This scaling parameter gives a good indication of how the surfaces of constant refractive index gradient are distributed. Large values of r_h will correspond to short structures along the ray path, whereas small values would compare to local spherical symmetry. This parameter is also related to the aspect ratio of the GWs, which determines the ratio of the horizontal to the vertical wavelength. This ratio is defined by the dispersion relation that characterizes GW propagation in the atmosphere, and its value, for the amplitude of the perturbation considered, varies generally between about 10 and 100 or more [Andrews *et al.*, 1987].

Figure 5 shows the profiles, over a range of one λ_v , of the refractivity perturbation (dotted lines) and the retrieved refractivity perturbation (solid lines) in the middle stratospheric region, given relative to the mean refractivity. This comparison was performed for four values of r_h to cover the range of GW spatial scales. We find that the GW perturbation, with the right wavelength and amplitude, appears explicitly in the retrieved refractivity for all four profiles. For the smallest r_h , the two profiles display striking similarities in phase and amplitude, confirming the total coherence of long horizontal waves with the condition imposed by the spherical symmetry assumption. For values of r_h larger than approximately 1, the phase of the perturbation begins to observe a shift, which increases with increasing r_h . With this phase shift is also associated a reduction in the amplitude of the perturbation. We notice, for instance, that for the largest of the considered values for r_h , the perturbation has almost disappeared from the retrieved refractivity profile, as its amplitude drops down to about 15% of the original perturbation amplitude.

As an illustration of what is most likely taking place when periodic gradients are present along the ray path, let us consider the simple representation of the layered atmosphere shown in Figure 6. The gravity wave field breaks the spherical symmetry imposed by the layering of the atmosphere in such a way that the surfaces of constant height (concentric layers) and the surfaces of constant refractivity gradient (dotted curves) are dissociated and do not overlap anymore. For the sake of clarity, we have exaggerated this effect in Figure 6. In this figure, the positive and negative marks indicate the sign of the refractivity gradient perturbation associated with the GW. Because the ray bending is a second-order

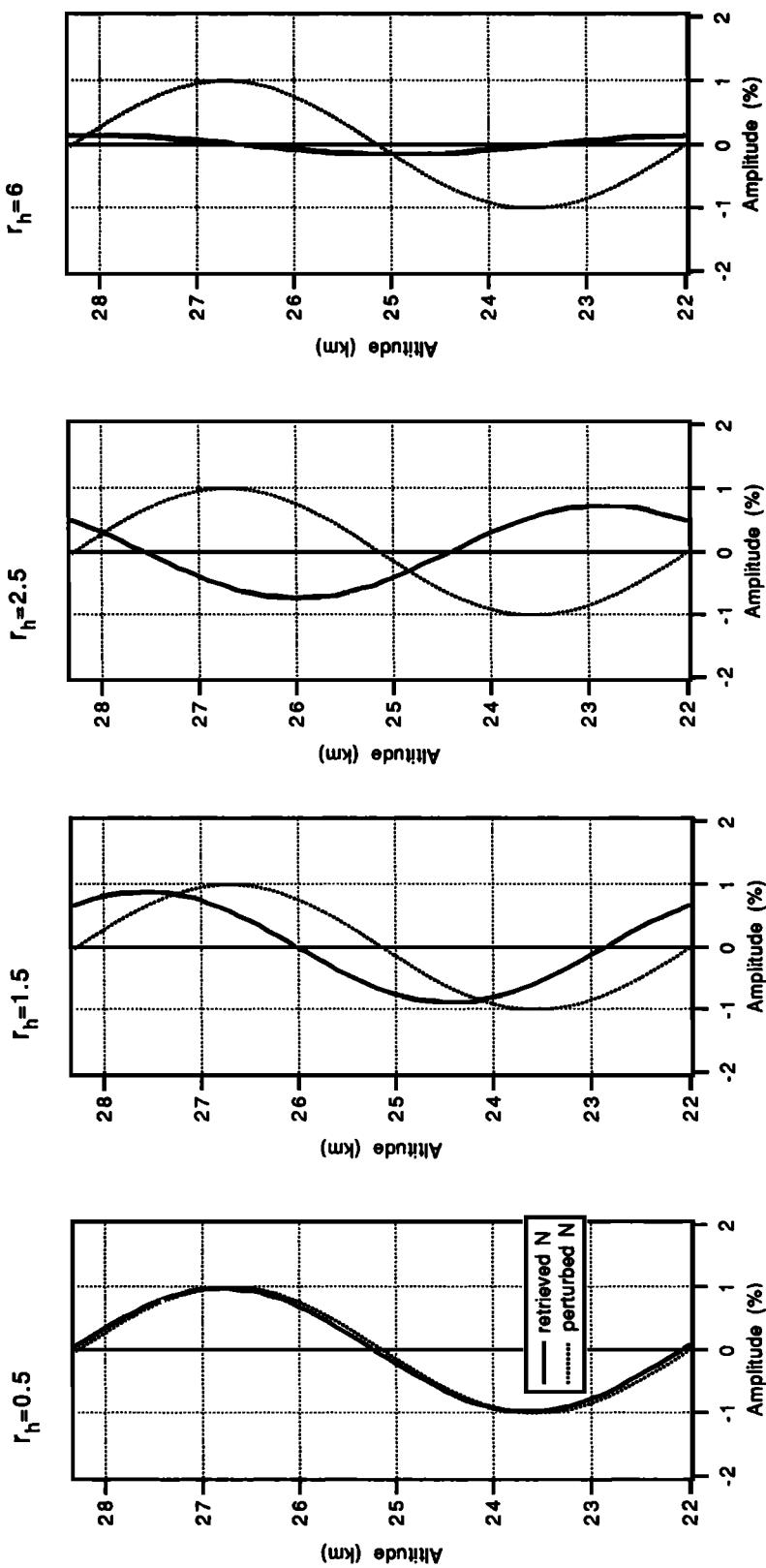


Figure 5. Comparison between the retrieved refractivity perturbation profile (solid lines) estimated over one vertical wavelength and the refractivity perturbation for four values of r_h (see text for definition) in the middle stratospheric region.

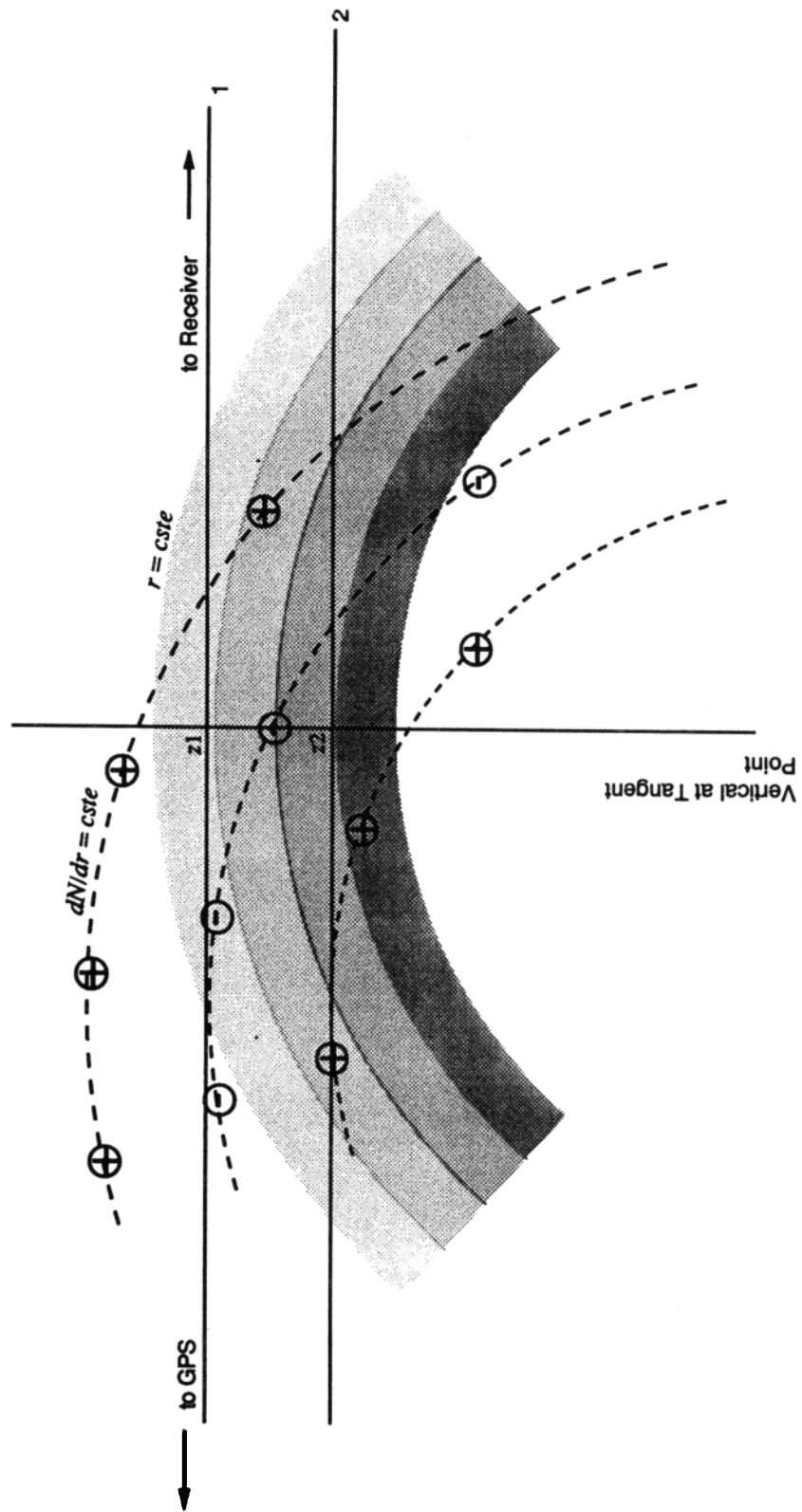


Figure 6. Sketch of the layered atmosphere showing the rays through a structure where the constant refractivity gradient surfaces (dotted curves) and the constant radius surfaces are dissociated.

effect, it is only sensitive to the refractivity gradient along the path, so that it experiences the strongest contribution from the layer where it becomes tangent to a surface $dN/dr = cste$. As a consequence, the rays would carry the perturbation signature (the phase, for instance) of the layer in which they are tangent to a surface $dN/dr = cste$ rather than the perturbation signature of the layer in which they are tangent to a surface $r = cste$. The magnitude of the tilt of the $dN/dr = cste$ surfaces with respect to the local horizontal translates therefore into an offset of the retrieved phase relative to the phase of the perturbation at the vertical of the ray tangent point. This could be the case, for instance, for rays 1 and 2 in Figure 6. To their respective altitudes of closest approach, z_1 and z_2 , would correspond a given phase of the perturbation while they would have passed at grazing incidence through a surface $dN/dr = cste$ in a layer with a different phase of the perturbation (one layer above, in this example). Now, as the $dN/dr = cste$ surfaces are modulated according to the vertical structure of the perturbation, it is clear that the earthward sinking of the ray perigee across the total thickness of the atmosphere, as the receiver sets behind Earth's horizon, will lead to a similarly periodic behavior of the retrieved refractivity perturbation at the vertical of the tangent point.

The relative tilt of the two curve systems is primarily a function of the spatial characteristics of the wave field, so that at fixed vertical wavelength, the tilt and therefore the phase shift between the retrieved refractivity and the perturbation profile will increase as the horizontal wavelength decreases. At the same as time λ_h decreases, the number of wavelengths encountered by the ray around the geometric tangent point will increase and a statistical averaging of the perturbation occurs for the short horizontal wavelengths. This is what we see in Figure 5, for instance, as the value of r_h is increased.

Conclusions

Profiles of neutral atmosphere parameters retrieved by limb measurements depend on the local atmospheric stratigraphy. Rays traveling through the layered atmosphere experience most of their bending during the last few kilometers before perigee, and since density fluctuations occurring over similar scales are introduced by GW activity, these fluctuations are likely to play a major role in affecting the accuracy of the retrieved profiles if spherical symmetry is assumed.

We have shown that the spherical symmetry assumption during the retrieval of the refractivity profiles in the presence of GWs could lead to discrepancies with the local refractivity profiles. Depending on the spatial characteristics of the GWs, the rays linking the source to a receiver will encounter local

refractivity gradients other than those expected from a stratified atmosphere, and the retrieval process assuming spherical symmetry is able to reproduce the vertical structure of the GWs at the vertical of the tangent point. It was shown that the presence of medium-scale waves, typically with aspect ratios of less than 100, produce a phase shift of the existing perturbation during the inversion. The largest deviation between the retrieved refractivity and the original perturbation at the vertical of the tangent point will be achieved when the two profiles are in phase opposition. This error will amount to twice the perturbation amplitude at altitudes where the perturbation phase corresponds to an amplitude maximum. Amplitudes of 1% in the density perturbation at these altitudes will mean about 3.5 to 4 K error in the lower stratosphere for the retrieved temperature.

These results raise, at the same time, the issue of the definition of the horizontal resolution in occultation measurements. It is clear that if the comparisons were performed over a extended horizontal distance of typically 350 km, corresponding to the horizontal resolution generally admitted for radio occultation, then the influence of the GWs would be attenuated.

It should also be emphasized that this analysis shows that a study of the global energy distribution of the medium- to large-scale gravity wave field from measurement data of the retrieved temperature profiles is possible since the perturbations produced by these waves will have their amplitude and their vertical wavelength preserved during the retrieval process, even if spherical symmetry is assumed. We should also mention the fact that these results are not restricted to radio occultation observations but should also be valid for occultation experiments aimed at deriving the vertical profiles of density and constituent concentrations from the measurement of the electromagnetic signal attenuation such as those that solar or stellar occultation experiments provide.

Acknowledgments. This work was partially supported by a grant from the European Space Agency.

References

- Allen, S. J., and R. A. Vincent, Gravity wave activity in the lower atmosphere: Seasonal and latitudinal variations, *J. of Geophys. Res.*, **100**, 1327, 1995.
- Andrews, D., J. R. Holton, and C. B. Leovy, *Middle Atmosphere Dynamics*, San Diego, Calif., 1987.
- Balsley, B. B., W. L. Ecklund, and D.C. Fritts, VHF echoes from the high-latitude mesosphere and lower thermosphere: Observations and interpretations, *J. Atmos. Sci.*, **40**, 2451, 1983.
- Fjeldbo, G., and R. Von Eshelman, The atmosphere of Mars analyzed by integral inversion of the Mariner

- IV occultation data, *Planet. Space Sci.*, **16**, 1035, 1968.
- Fjeldbo, G., A. Kliore, and R. Von Eshelman, The neutral atmosphere of Venus as studied with the Mariner V Radio Occultation Experiments, *Astron. J.*, **76**, 123, 1971.
- Gorbunov, M. Y., Solution of inverse problems of remote atmospheric refractometry on limb paths, *Izv. Atmos. Oceanic Phys.*, Engl. Transl., **26**(2), 86, 1990.
- Kursinski, E. R., et al., Initial results of radio occultation observations of Earth's atmosphere using the Global Positioning System, *Science*, **271**, 1107, 1996.
- Lindal, G. F., The atmosphere of Neptune : An analysis of radio occultation data acquired with Voyager 2, *Astron. J.*, **103**, 967, 1992.
- Lindal, G. F., G. E. Wood, H. B. Hotz, D. N. Sweetnam, R. Von Eshelman, and G. L. Tyler, The atmosphere of Titan: An analysis of the Voyager I radio occultation measurements, *Icarus*, **53**, 348, 1983.
- Lindal, G. F., J.R. Lyons, D. N. Sweetnam, R. Von Eshelman, D. P. Hinson, and G. L. Tyler, The atmosphere of Uranus: Results of radio occultation measurements with Voyager 2, *J. Geophys. Res.*, **92**, 14987, 1987.
- Lusignan, B., G. Modrell, A. Morrison, J. Pomalaza, and S. G. Ungar, Sensing the Earth's atmosphere with occultation satellites, *Proc. IEEE*, **57**, 458, 1969.
- Rangaswamy, V., Recovery of atmospheric parameters from the Apollo/Soyuz-ATS-F radio occultation data, *Geophys. Res. Lett.*, **3**(8), 483, 1976.
- Roble, R. G., and P. B. Hays, A technique for recovering the vertical number density profile of atmospheric gases from planetary occultation data, *Planet. Space Sci.*, **20**, 1727, 1972.
- Vincent, R. A., and I. M. Reid, HF Doppler measurements of mesospheric gravity wave momentum fluxes, *J. Atmos. Sci.*, **40**, 1321, 1983.
- Wilson, R., A. Hauchecorne, and M.-L. Chanin, Gravity wave spectra in the middle atmosphere as observed by Rayleigh lidar, *Geophys. Res. Lett.*, **17**(10), 1585, 1990.

M.B. Belloul and A. Hauchecorne, Service d'Aéronomie, Centre National de la Recherche Scientifique, BP 3, 91371, Verrières le Buisson, France.
(e-mail: belloul@aerov.jussieu.fr)

(Received April 3, 1996; revised October 28, 1996;
accepted November 11, 1996.)